ICRC'07

Mérida, México

Observations of Very High Energy Gamma-Rays during Moonlight and Twilight with the MAGIC Telescope

JAVIER RICO[1], EMMA DE OÑA-WILHELMI[1],JUAN CORTINA[1], ECKART LORENZ[2] FOR THE MAGIC COLLABORATION

[1]*Institut de Fisica d'Altes Energies, Barcelona, Spain*
[2]*Max-Planck-Institut für Physik, München, Germany*
jrico@ifae.es, emma@ifae.es

Abstract: We study the capability of the MAGIC telescope to observe under moderate moonlight. TeV γ-ray signals from the Crab nebula were detected with the MAGIC telescope during periods when the Moon was above the horizon and during twilight. This was accomplished by increasing the trigger discriminator thresholds. No change is necessary in the high voltage settings since the camera PMTs were especially designed to avoid high currents. We characterize the telescope performance by studying the effect of the moonlight on the γ-ray detection efficiency and sensitivity, as well as on the energy threshold.

Introduction

Ground-based searches for very high energy (VHE) γ-ray emission from celestial objects are normally carried out by so-called imaging air Cherenkov telescopes (IACT) during clear, moonless nights. If such a strict requirement is relaxed to allow observations under moderate moonlight or twilight, an increase of the duty cycle to 18% (from $\sim$1000 to $\sim$1500 hours of observations per year) is possible. VHE observations under moonlight have been tested in the past [8, 4, 6] but with solutions that were too expensive, time consuming and not efficient in terms of energy threshold and sensitivity. The MAGIC IACT [7] has been designed to carry out observations also during moderate moonlight. This places MAGIC in a prominent position, in particular for the study of variable sources as well as in multi-wavelength campaigns together with other instruments. In this paper we describe the technical innovations and analysis changes that allow observations in the presence of the Moon with MAGIC.

Traditionally, PMTs are operated with amplification gains around $10^6 - 10^7$ which, under moonlight, generate continuous (direct) currents (DCs) that can damage the last dynode, resulting in rapid ageing of the PMT. MAGIC PTMs run at a gain of about 3×10^4 [2]. In order to also detect single photoelectrons (phe) the PMT signal is fed to an AC-coupled fast, low noise preamplifier to raise the combined gain to about 10^6. The PMT analog signal is transmitted over an optical fiber, converted into an electrical pulse and split into two branches, one of which enters a discriminator (DT), which issues a digital signal whenever the pulse exceeds a given threshold.

The increase of the background light due to the presence of the Moon depends on various factors including Moon and source zenith angles, Moon phase, angular distance to the Moon and atmospheric conditions. At around $25°$ away from the Moon the direct scattered moonlight approaches a constant level below that of the night sky light background. Figure 1 shows the dependence of the trigger rate (for a four neighboring pixels configuration) on the DT settings, for different illumination conditions (which produce different anode currents in the camera). The light of night sky (LONS) is responsible for the steep increase at low DT values (at $\sim$30 a.u. in the case of dark observations). At higher DT values the rate is caused mostly by Cherenkov showers. The telescope operates at the minimum possible DT for which the contribution of accidental triggers is negligible. For extragalactic regions (DC=1μA) the DTs are
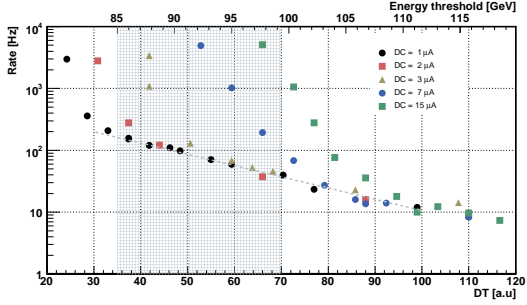
Figure 1: Trigger rate as a function of the discriminator threshold for four neighboring pixels configuration and different camera illuminations. The shaded area shows the range used for MAGIC regular observations (dark and under moonlight). The dashed line shows the linear regime. The upper axis shows the corresponding energy threshold (after image cleaning) for observations at zenith angles between 20° and 30° as deduced in Section 3.

generally set to 30 a.u., which corresponds to a pulse charge of 8-10 phe. Higher DT values are needed to keep the trigger rate below the limit of the DAQ system (500 Hz) for observations during twilight and moonlight. We restrict MAGIC observations to a maximum DC of 8 μA. This permits observations in the presence of the Moon until (since) 3-4 days before (after) full Moon, for an angular distance to the Moon greater than 50° [2].

Observations and Data Analysis

To characterize the response of the telescope under moonlight, we observed the Crab nebula at different light conditions (including dark observations used as reference) between January and March 2006, in the ON/OFF mode. Two data sets, one with zenith angle between 20° and 30°, and a second one between 30° and 40°, were acquired and analyzed separately. Depending on the different moonlight levels, the resulting anode currents ranged between 1 and 6 μA. Correspondingly, the DT was varied between 35 and 65 units. The acquired data were processed by the standard MAGIC analysis chain [1]. The images were cleaned using absolute tail and boundary cuts at 10 and 5 phe, respectively. Quality cuts
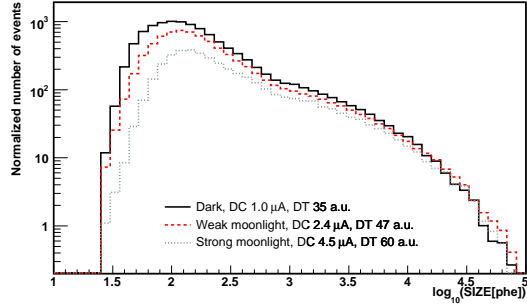

Figure 2: Distributions of SIZE before analysis cuts for three Crab nebula samples acquired under different light conditions. The histograms have been normalized to a common observation time. Note that the distributions are completely dominated by hadronic events ($\sim 99\%$).

based on the trigger and after-cleaning rates were applied in order to remove bad runs. The shower images were parameterized using the Hillas parameters [5] SIZE, WIDTH, LENGTH, DIST, CONC and ALPHA, combined (except for the latter) into an adimensional variable (HADRONNESS) for γ/hadron separation by means of a Random Forest classification algorithm [3]. The signal region was defined by the cuts HADRONNESS<0.15 and ALPHA<8°.

Results

As we increase the DT levels to counteract accidental triggers, one depletes the SIZE distribution of shower candidates, as expected, mostly at low values. However, we find that a substantial number of showers with SIZE up to 10^4 phe, i.e. those well above the trigger level (which is around 50 phe), are also suppressed (see Figure 2). On the other hand, the LENGTH, WIDTH and CONC distributions above 200 phe do not show significant differences (See Figure 3) and therefore we do not expect γ/hadron separation to degrade due to the presence of the Moon. Below 200 phe the distributions are distorted by the different trigger threshold.

The supressed high-SIZE showers are those at high DIST (see Figure 3c), corresponding to a high impact parameter, where a significant fraction of the
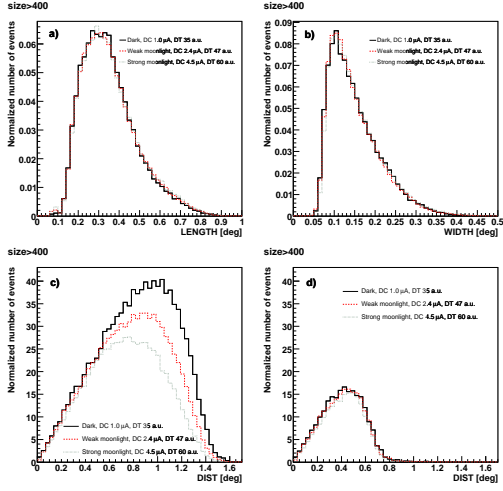
Figure 3: Distributions of LENGTH (a), WIDTH (b) and DIST for all recorded events (c) and for images fully contained in the inner camera (d) for SIZE>400 phe. Three Crab nebula samples acquired under different moonlight conditions. The histograms are normalized to a unit area in (a) and (b) and to a common observation time in (c) and (d).
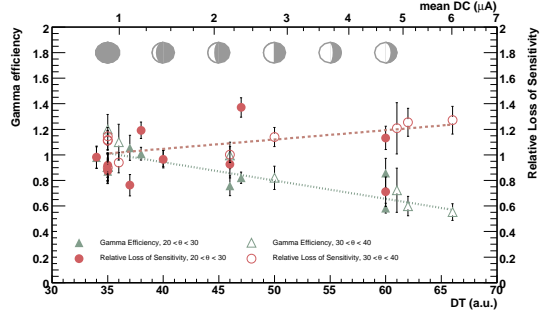

Figure 4: Relative γ-ray detection efficiency (green triangles, left axis) and sensitivity (red circles, right axis) as a function of DT (SIZE> 400 phe), for zenith angle bins $[20°, 30°]$ (filled markers) and $[30°, 40°]$ (empty markers) measured from Crab nebula observations.
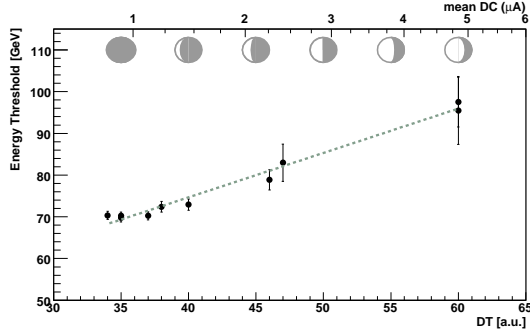

Figure 5: Energy threshold after image cleaning as a function of DT obtained from MC simulated γ-ray events (for zenith angle between $20°$ and $30°$). The top axis shows the typical mean DC for a chosen DT value.

light falls outside the trigger area ($1°$ radius around the camera center). In some cases, the fraction of the shower image contained in the trigger area does not exceed the increased threshold for at least 4 neighboring pixels, as required for a trigger. A confirmation of this hypothesis was obtained by two different tests. First, the DIST distributions for events fully contained in the trigger region were compared (Figure 3d). In such a case we find similar distributions. The second test was performed by observing Crab in dark conditions (DC~1.1 μA), but with increased DTs. In this case we found similar inefficiencies as those shown in Figure 3c). Therefore we can conclude that the change of the DIST distribution is not related to the mean DC current (i.e. with the camera illumination) but only to the DT level.

These results show that moonlight does not distort the images from Cherenkov showers and therefore the analysis based on the Hillas parameters does not have to be adapted for data acquired under moonlight, and in particular the γ/hadron separa-

tion power is not reduced for this kind of observations. In addition, the differences that we find in the event rates and the DIST distributions are exclusively due to the fact that the DTs were increased to keep a low rate of accidental events, together with the fact that the trigger area does not span the whole camera. With a faster DAQ system one could have a fix DT level and deal with the extra noisy events introduced by the moonlight during the offline analysis.

For this study the dependence of the telescope response on the level of Moon illumination will be parameterized as a function of DT. As is shown in Figure 2, there is a reduction in the collection area over a wide range of energies. We use Crab

nebula observations to parametrize the efficiency of detecting γ-rays, for every DT and SIZE, relative to the values for dark observations. These values are used during the off-line analysis together with the MC simulation with standard DTs to calculate the correct collection areas. For this, the observations of the Crab nebula are divided into different samples according to the observation date, SIZE and DT values. For each of the samples we get a measurement of the γ-ray rate (R) and sensivity (s). We find that, for a given SIZE range, the dependences of R/R_0 and s/s_0 with the DT are well described by linear functions $(R/R_0, s/s_0 = (1 - S_{R,s}(DT - DT_0)))$, where R_0, s_0 and DT_0 are the rate, sensitivity and DT values, respectively, for the dark observation case. $S_{R,s}$ are let free during the fit and are referred to as efficiency/sensitivity loss rate, respectively. The results for SIZE>400 phe and the two considered zenith angle samples ($[20°, 30°]$ and $[30°, 40°]$) are shown in Figure 4. The fit parameters obtained for both zenith angles are compatible within statistical errors. This allows us to perform a combined fit for both samples. For SIZE>400 phe we obtain the following expression for the γ-ray efficiency and sensitivity:

$$\begin{aligned} R/R_0 &= 1 - (1.41 \pm 0.32) \times 10^{-2}(DT - DT_0) \\ s/s_0 &= 1 + (6.3 \pm 1.6) \times 10^{-3}(DT - DT_0) \end{aligned}$$

In order to understand the dependence of the γ-ray detection efficiency on the energy we have performed the same study for four bins of SIZE, namely [200,400], [400,800], [800,1600] and [1600,6400] phe, which roughly correspond to the energy ranges [150,300], [300,600], [600-1000] and > 1000 GeV, respectively, for low zenith angle. Up to SIZE=3000 phe we find a linear dependence that can be parameterized by:

$$\begin{aligned} S_R &= (2.24 \pm 0.13) \times 10^{-2} \\ &\quad -(7.2 \pm 1.2) \times 10^{-6} \text{ SIZE [phe]} \\ S_s &= (1.63 \pm 0.14) \times 10^{-2} \\ &\quad -(7.4 \pm 1.8) \times 10^{-6} \text{ SIZE [phe]} \end{aligned}$$

We tested the dependences of these results on different HADRONNESS and ALPHA cuts, obtaining in all cases similar results.

Finally, it is important to understand the influence of the moonlight on the energy threshold. We de-fine the energy threshold as the peak of the energy distribution of all events after image cleaning and before analysis cuts. The dependence of the energy threshold is well described by the following linear function (see Figure 5):

$$\frac{E_{\text{th}}}{\text{GeV}} = (69.3 \pm 0.4) + (1.06 \pm 0.03)(DT - DT_0)$$

This increase is relatively marginal, and it has to be noted again that it is due to the increase of the DTs, and hence only indirectly to the increase in the camera illumination.

References

[1] J. Albert and et al. Signal Reconstruction for the MAGIC Telescope. *ArXiv Astrophysics e-prints*, December 2006.

[2] A. Armada. Characterization and some applications of the anode current monitoring system of the MAGIC telescope. *Master Thesis*, 2005.

[3] L. Breiman. Random Forests. *Machine Learning*, 45:5–32, 2001.

[4] M. Chantell and et al. Gamma-Ray Observations in Moonlight with the Whipple Atmospheric Cherenkov Hybrid Camera. In *International Cosmic Ray Conference*, volume 2 of *International Cosmic Ray Conference*, pages 544–+, 1995.

[5] A. M. Hillas. Cerenkov light images of EAS produced by primary gamma. In F. C. Jones, editor, *International Cosmic Ray Conference*, volume 3 of *International Cosmic Ray Conference*, pages 445–448, August 1985.

[6] D. Kranich and et al. TeV gamma-ray observations of the Crab and MKN 501 during moonshine and twilight. *Astroparticle Physics*, 12:65–74, October 1999.

[7] E. Lorenz. Status of the 17-m magic telescope. *New Astron. Rev.*, 48:339–344, 2004.

[8] E. Pare and et al. Image Shapes of Showers in UV and Visible Cherenkov Light. In *International Cosmic Ray Conference*, volume 1 of *International Cosmic Ray Conference*, pages 492–+, August 1991.